

## FINDING CALIBRATOR STARS FOR OPTICAL INTERFEROMETRY VISIBILITY MEASUREMENTS

A.F. Boden<sup>1</sup>

**Abstract.** By construction, optical (and near-infrared) interferometers typically have resolutions designed to resolve stellar and circumstellar features. Therefore gaging the point-source response of the interferometer in its operating environment is critical to the scientific interpretation of data from these devices. This is typically performed with observations of calibration sources that are modeled to be simple and quasi-unresolved by the interferometer. Herein I will discuss the goals and strategies for and issues with the selection of objects to serve as calibration sources for optical interferometry visibility measurements.

### 1 Introduction – Objectives in Selecting Calibration Sources

As discussed in other chapters in this volume, an astronomical interferometer is a device that measures the interference (or attributes associated with the interference) of radiation from astronomical sources. In most applications we use the interferometer to measure the amount of interference (or coherence) in the incident radiation field to obtain information about the source morphology on angular scales sampled by the interferometer. In this context it is critical to gage the imperfect response (i.e. the degree of incoherence) of the device in its operating environment (e.g. in the turbulent atmosphere).

Similar to other observational techniques, the degree of instrument incoherence is typically estimated by quasi-contemporaneous measurement of *calibration sources* – astronomical sources that are used to derive a model of the instrument response. The phenomenon that effect instrument performance are many and varied, but in general are variable as a function of time and sky location. Therefore, calibration sources are typically geometrically similar to the target (i.e. nearby in the sky) for both observational efficiency and instrumental and atmospheric variation reasons. In most interferometric applications the calibration model is

---

<sup>1</sup> Interferometry Science Center, California Institute of Technology, Pasadena, CA

taken to be linear and assumes the form of a *system visibility*  $V_{sys}$ , or the point-source response of the interferometer. This system visibility is multiplicatively applied to visibility measurements made on the target of interest to estimate the measurements made by an ideal interferometer <sup>1</sup>:

$$V_{sys} \approx V_{cal-meas}/V_{cal-exp}$$

and

$$V_{targ} \approx V_{targ-meas}/V_{sys} = V_{targ-meas}V_{cal-exp}/V_{cal-meas} \quad (1.1)$$

The reader interested in more detailed information on calibration techniques is referred to Mozurkewich *et al.* (1991) and Boden *et al.* (1998).

The title of this contribution suggests that pragmatically some astronomical objects are better suited to serve as interferometer calibration sources than others. For the purposes of this discussion we will confine our attention to stars as calibration sources; this is both conventional and appropriate given that much work in optical interferometry concentrates on stellar astrophysics. Generally speaking, the attributes of good calibration stars can be inferred from the form of Eq. 1.1. Calibration errors enter Eq. 1.1 both through the expected visibility on the calibration star  $V_{cal-exp}$  and through the calibration observation noise properties; the variance from such calibration errors have the generic form:

$$\sigma_{V-targ}^2 \propto V_{cal-exp}^2 \frac{\sigma_{V-cal-meas}^2}{V_{cal-meas}^2} + \left( \frac{\partial V_{cal-exp}}{\partial model} \right)^2 \sigma_{model}^2 \quad (1.2)$$

The first of these terms describes the fractional uncertainty on the calibrator observations, presumably a question of observation SNR, and requires the star to be sufficiently bright. The second term describes our ability to correctly predict the expected visibility on the calibration star. Therefore, operationally a good calibration star yields a small net calibration error by striking a balance in simultaneously mitigating the contribution from both terms in Eq. 1.2.

In practice the second term in Eq. 1.2 can be minimized either by minimizing the fundamental uncertainty in the model parameters ( $\sigma_{model}$ ), or by minimizing the sensitivity of the calibration on the model parameters – i.e. minimizing  $|\partial V_{cal-exp}/\partial model|$ . To illustrate, it is typical to model the calibration star as a uniform disk of apparent diameter  $\Theta$ :

$$V_{cal-exp} = \frac{2J_1(\pi\Theta B_{\perp}/\lambda)}{\pi\Theta B_{\perp}/\lambda} \quad (1.3)$$

with  $J_1$  is the first-order Bessel function,  $B_{\perp}$  is the interferometer baseline length perpendicular to the star direction, and  $\lambda$  is the interferometer operating wavelength (Fig. 1; see Boden 1999 for a derivation). As we lack a direct diameter

---

<sup>1</sup>The calculations are illustrated in visibility space, but optical/near-infrared interferometers typically work in visibility-squared space for noise statistics reasons.

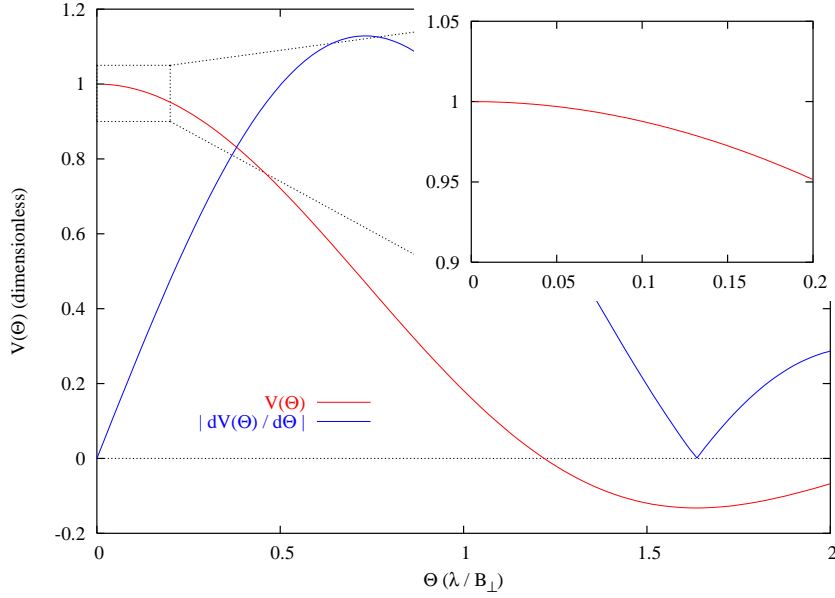


**Fig. 1.** Disk Visibility and Derivative. The predicted visibility  $V$  of a uniform disk as a function of its apparent diameter  $\Theta$  (Eq. 1.3) and the first derivative  $|dV/d\Theta|$  are given.  $\Theta$  is in units of the projected interferometer fringe spacing  $\lambda/B_{\perp}$ . Inset is a closeup of the unresolved limit ( $\Theta \ll \lambda/B_{\perp}$ ) where  $V \rightarrow 1$  and  $|dV/d\Theta| \rightarrow 0$ . Calibration sources are typically chosen to be as unresolved as possible so as to minimize systematic calibration error from finite knowledge of  $\Theta$  and large values of  $|dV/d\Theta|$ .

measurement for all but a few stars, the dominant source of error in applying Eq. 1.3 in Eq. 1.2 is a limited knowledge of the estimated calibrator diameter  $\Theta$  (characterized by  $\sigma_{\Theta}$ ; see §2). This motivates choosing calibrators that have small  $|dV/d\Theta|$ , i.e. as illustrated in Fig. 1 are as unresolved as possible ( $\Theta \ll \lambda/B_{\perp}$ ).

The basic tasks in selecting calibration sources for a proposed science experiment is to identify possible sources that could be efficiently observed in conjunction with the target, and to select those sources that have attributes that lead to accurate calibration. The first of these is fundamentally a geometric issue; what objects are within some set of geometric constraints of the science target. The second of these involves understanding the astrophysics of potential calibrators so as to select those likely to have desirable characteristics. In what follows I will discuss several pragmatic aspects to the calibration selection, namely the estimation of stellar angular diameters from ancillary data (§2), the identification of multiplicity (§3), and observational plans and strategies leading to robust calibrations (§4).

## 2 Estimating Stellar Angular Diameters

As argued above, we are motivated to consider stars that are unresolved by the interferometer. But because astronomical distances are large, stellar apparent sizes are small. For instance, our own sun viewed from a typical solar neighborhood distance of 10 pc is less than 1 milliarcsecond ( $10^{-3}$  arcseconds, mas) in apparent diameter. Therefore, as an adjunct to both selecting and using calibration stars, it is a practical necessity to estimate stellar angular diameters from ancillary data. While many techniques exist for such estimates, the most broadly applicable and prevalent techniques are based on modeling the stellar photosphere as a blackbody, in which case the apparent diameter of the star reduces to a simple function the observed bolometric flux and the effective temperature (e.g. see Blackwell & Lynas-Gray 1994 and references therein). Given the tutorial nature of these proceedings it is instructive to include the derivation of this fundamental result here.

First consider a unit area Plank blackbody at temperature  $T$ . The *emittance* (radiation emitted per unit surface – dimensions of energy per unit time) is:

$$\mathcal{F} = \sigma T^4 = \pi \int_0^\infty d\lambda B_\lambda(T) = \pi \int_0^\infty d\lambda \frac{2hc^2/\lambda^5}{\exp(hc/\lambda kT) - 1}$$

where the last two expressions capture the spectral energy distribution of the blackbody radiation. Radiation from the unit surface is isotropic, so the *specific intensity* (radiation flux density per unit solid angle – dimensions of energy per unit time per unit solid angle) is a simple function of the projected area, so in a direction  $\hat{o}$  this flux density is:

$$I \equiv \frac{d\mathcal{F}}{d\Omega} = \frac{\sigma T^4}{\pi} \hat{\mathbf{n}} \cdot \hat{\mathbf{o}} = \frac{\sigma T^4}{\pi} \cos \theta = \cos \theta \int_0^\infty d\lambda B_\lambda(T)$$

where  $\hat{\mathbf{n}}$  is the unit normal to the surface, and  $\theta$  is the angle between  $\hat{\mathbf{n}}$  and  $\hat{\mathbf{o}}$ . Thus at a location  $D \hat{\mathbf{o}}$  from the unit emitter, the radiation flux per unit cross-sectional area (dimensions of energy per unit time per unit area) is:

$$f_a = \frac{d\mathcal{F}}{d\Omega} * \Omega = \frac{d\mathcal{F}}{d\Omega} / D^2 = \frac{\sigma T^4}{\pi D^2} \cos \theta = \frac{\cos \theta}{D^2} \int_0^\infty d\lambda B_\lambda(T) \quad (2.1)$$

Now consider the photosphere of a star as an isotropic sphere of radius  $R$ , the surface of which is taken to be a Plank blackbody radiator at uniform temperature  $T$ . For the observer at distance  $D$  the total radiation flux per unit cross-sectional area (the *bolometric flux*) can be computed as the integral of the contributions  $f_a dA$  over the hemisphere of the star visible to the observer:

$$F_{bol} = \int_{2\pi} dA f_a = \int_{2\pi} dA \frac{\sigma T^4}{\pi D^2} \cos \theta = \int_{2\pi} dA \frac{\cos \theta}{D^2} \int_0^\infty d\lambda B_\lambda(T)$$

Choosing the observer direction  $\hat{\mathbf{o}}$  as the reference axis in a spherical polar coordinate system allows us to identify the star surface area element  $dA$  as  $R^2 \sin \theta d\theta d\phi$ ,

making the evaluation of the integral straightforward:

$$F_{bol} = \frac{R^2 \sigma T^4}{\pi D^2} \int_0^{2\pi} d\phi \int_0^{\pi/2} d\theta \sin \theta \cos \theta = \frac{1}{4} \frac{4R^2}{D^2} \sigma T^4 = \frac{1}{4} \Theta^2 \sigma T^4 \quad (2.2)$$

$$F_\lambda = \frac{1}{4} \pi \Theta^2 B_\lambda(T) = \frac{\pi \Theta^2}{4} \frac{2hc^2/\lambda^5}{\exp(hc/\lambda kT) - 1} \quad (2.3)$$

with the identification of the star's angular diameter  $\Theta = 2R/D$ , and introducing the stellar flux per unit wavelength  $F_\lambda$ . Solving Eq. 2.2 for  $\Theta$  yields the desired angular diameter estimator:

$$\Theta = \sqrt{\frac{4F_{bol}}{\sigma T^4}} \approx 8.17 \text{ mas} \times 10^{-0.2*(V+BC)} [T/5800 \text{ K}]^{-2} \quad (2.4)$$

with  $V$  and  $BC$  as the star's (Johnson) visual magnitude and bolometric correction respectively. A couple of aspects of Eq. 2.4 are noteworthy. First, it is significant that no particular knowledge of the physical size of the star is necessary – the bolometric flux characterizes the solid angle of the star on the sky, and the blackbody temperature characterizes the emittance of the stellar surface. This emphasizes the intuitive notion that two stars of the same temperature but different physical radii  $R_1$  and  $R_2$  (e.g. an M-dwarf and an M supergiant) will have the same apparent size and bolometric flux so long as  $R_1/D_1 = R_2/D_2$ . Secondly, in deriving Eq. 2.4 it was sufficient that the photospheric emittance was taken as isotropic and characterizable by a ancillary parameter (temperature); no particular use is made of the blackbody SED model.

A quick quantitative example is in order – consider the sun. Cox *et al.* (1999) lists the sun's radius as  $6.955 \times 10^{10}$  cm, so at a distance of 10 pc the true apparent diameter of the sun would be 0.930 mas. Estimating the apparent diameter by Eq. 2.4, the absolute bolometric magnitude of the sun is 4.74 ( $3.15 \text{ erg s}^{-1} \text{ cm}^{-2}$ ), and its *effective* temperature is 5777 K (Cox *et al.* 1999), which yields an apparent angular diameter of 0.921 mas, an agreement of better than 1%! This agreement is not nearly as remarkable as it sounds; Eq. 2.2 operationally *defines* the effective temperature of a star – the temperature of a blackbody of the same physical size and bolometric luminosity (Rybicki & Lightman 1979). So in this example the sun's effective temperature is in fact computed from its physical size and bolometric luminosity.

The operational issue in applying Eq. 2.4 to potential calibrators is determining the bolometric flux and effective temperature for the star. The most prevalent methods for this estimation is by modeling the observed spectral energy distribution (SED) of the star. This is illustrated in Fig. 2 and 3 which depicts the modeling of SEDs for 51 Pegasi (HD 217014) and T Tauri (HD 284419) with a Plank blackbody form (specifically Eq. 2.3) with free parameters  $\Theta$  and  $T_{eff}$ . In both cases the flux data for the stars is derived from archival optical and infrared photometry. In the first example (Fig. 2) the 51 Peg SED is well-modeled by Eq. 2.3 with  $T \approx 5600$  K and  $\Theta \approx 0.77$  mas (despite the putative planetary-mass companion to 51 Peg; Mayor & Queloz 1995, Marcy *et al.* 1997); the implied

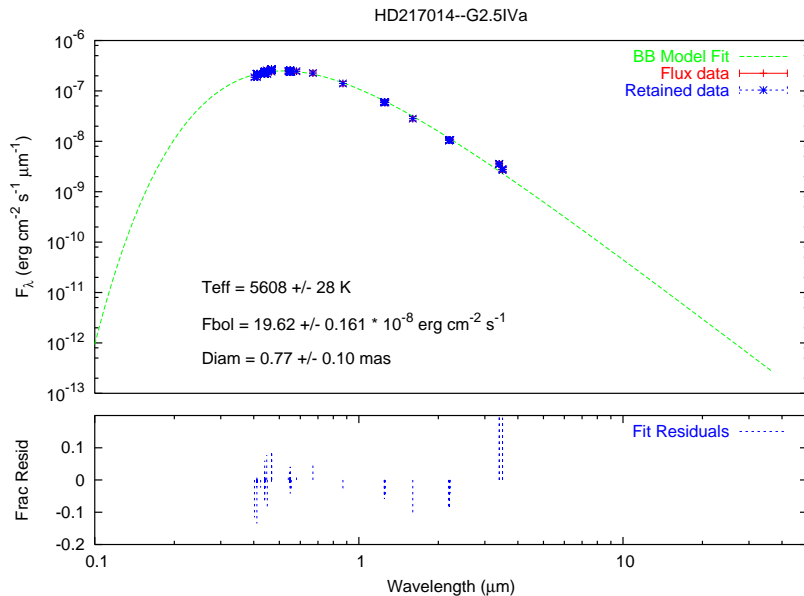


**Fig. 2.** Modeling of the spectral energy distributions for 51 Pegasi (HD 217014) with a single-temperature Plank blackbody photosphere model (Eq. 2.3). The agreement between data and model is reasonably good.

temperature and physical size ( $R \sim 1.3 R_{\odot}$  from this diameter estimate and Hipparcos parallax; ESA 1997) are in good agreement with the putative evolutionary state of the star. Conversely, the single-component model fit to T Tau in Fig. 3 illustrates a relatively poor agreement with the data, exhibiting a strong infrared excess. Presumably this is due to T Tau being a triple system (Koresko 2000), photometrically variable (Ghez *et al.* 1991), and possessing significant amounts of circumstellar material around at least two of the components inferred by SED modeling (e.g. Ghez *et al.* 1991) and direct detection IR interferometry (Akeson *et al.* 2000).

The poor agreement between model and data in Fig. 3 illustrates a second, related point. We typically apply the uniform disk model to calculate visibilities for calibration sources (Eq. 1.3) – implicitly assuming a simple single-temperature photosphere. In the case of T Tau we see a significant departure between this model and the observed photometry, attributable to both multiplicity and circumstellar material. This is especially true in the infrared, where the relative contributions of warm circumstellar material are more significant in comparison to the parent

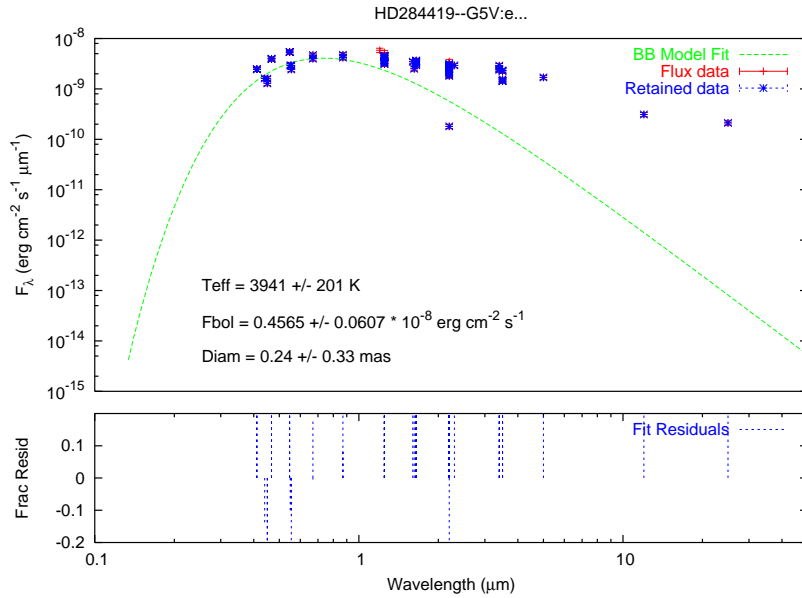


**Fig. 3.** Modeling of the spectral energy distributions for T Tau (HD 284419) with a single-temperature Plank blackbody photosphere model (Eq. 2.3). The agreement between the data and the model is considerably poorer than for 51 Peg (Fig. 2).

star, and many interferometers (e.g. PTI<sup>2</sup>, CHARA<sup>3</sup>, KI<sup>4</sup>, VLTI<sup>5</sup>) operate. Thus we see that in addition to facilitating angular diameter estimation, SED modeling can be an important tool in identifying possible visibility modeling problems with potential calibration sources. If a simple single-component SED model poorly predicts available photometric data, then it is a reasonable assumption that a simple single-disk visibility model will fail to predict observed visibilities.

### 3 Stellar Multiplicity

Binary stars are sufficiently prevalent that they have been described as “the vermin of the skies”. In the definitive study for solar-like stars Duquennoy & Mayor (1991, DM91) determined that roughly 1/2 of all primary stars had stellar companions, and similar statistics are thought to hold for other stellar types. From the standpoint of identifying potential visibility calibrators the prevailing wisdom

<sup>2</sup>see <http://huey.jpl.nasa.gov/palomar>

<sup>3</sup>see <http://www.chara.gsu.edu/CHARA/array.html>

<sup>4</sup>see <http://huey.jpl.nasa.gov/keck>

<sup>5</sup>see <http://www.eso.org/projects/vlti/>

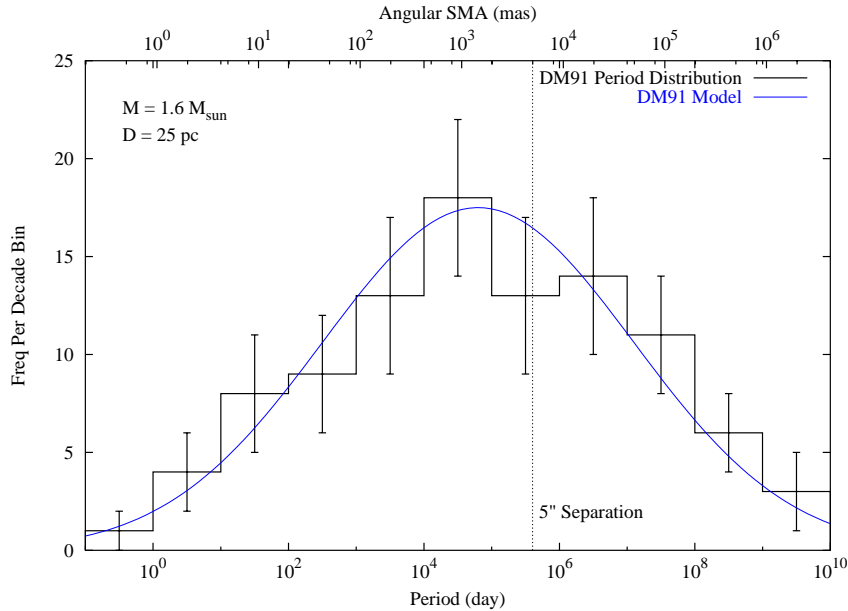


**Fig. 4.** Observed Period Distribution For Solar-Like Binary Stars (from Duquennoy & Mayor 1991). On the top horizontal axis we indicate the implied angular semi-major axis assuming a system mass of  $1.6 M_{\odot}$  and a distance of 25 pc. A dotted vertical line is given at  $5''$  (see text discussion).

is multiplicity is to be avoided. Surely this is an overstatement; simple visual binaries with separations of a few arcseconds or more pose no significant risk in application as calibrators. However, multiplicity over angular scales that would effect visibility measurements *should* be avoided – the modeling of visibilities from such systems (e.g. Eq. 1.2) excessively complicate the calibration process. Figure 4 depicts the observed DM91 binary period distribution (corrected for detection efficiency), and the log-normal analytical distribution model provided by DM91. For the purposes of the present discussion I have added a calculation of the implied angular semi-major axis assuming a typical system mass of  $1.6 M_{\odot}$  and system distance of 25 pc. If we were to exclude systems with projected separations of  $5''$  (the dotted vertical line in Fig. 4) or less we would exclude approximately 60% of the observed DM91 population.

In order to select potential calibrators, the operational question is how to identify multiplicity. Here there are no great pearls of wisdom beyond detective work. Some of the standard sources for the identification of binarity are: the SIMBAD stellar database hosted by Centre de Données astronomiques de Strasbourg<sup>6</sup>, vari-

<sup>6</sup>see <http://cdsweb.u-strasbg.fr/>

ous spectroscopic binary catalogs such as that by Batten<sup>7</sup> (1989), the Washington Double Star catalog<sup>8</sup>, and the Hipparcos astrometric catalog – in particular the orbital and component solution annexes<sup>9</sup> (ESA 1997).

## 4 Observing and Calibrating Visibilities

Once potential calibrators are identified for a particular experiment, it is then necessary to define the parameters for the observing, typically addressing such issues as the number of calibrators to be carried in the experiment, the relative ratio of calibration to science observations, and any specific order for the observations to proceed in. With regard to the number, a conventional rule of thumb is two calibrators carried through the experiment duration is a safe strategy. This allows extensive cross-checking between calibrators for consistency, and some redundancy in the event that one of the selected objects exhibit unexpected and/or unwanted features in the data. With regard to the ratio of science and calibration data, assuming that the instrument performs similarly on the target and calibrators, the optimal (i.e. minimum-variance on the calibrated observation SNR) ratio of target to calibrator data is 1:1. However, external operational objectives such as overall instrument science throughput may well override the desire to optimize the SNR on individual observations.

It is our experience at PTI that the overall best calibration performance results when target and calibration measurements are interleaved in short (e.g. < 15 min) cycle times – this amounts to the visibility analog of “chopping” between target and calibrator. These chop cycles allow the calibration model to be responsive to temporal variations in the instrument or environment (e.g. see Boden *et al.* 1998). Similarly the choice of calibrators near the target both serve to make the chop cycles more efficient and mitigate the effects of any sky position-dependent effects in either the instrument or atmosphere.

## 5 Summary

In this contribution I have introduced the concepts for selecting and evaluating possible calibration sources, and for observing calibration sources to produce well-calibrated visibilities. Most if not all of these techniques can be implemented in the context of observation planning software (for instance, the reader is referred to the documentation for the ISC’s *getCal* observation planning package at <http://isc.caltech.edu/software/getCal>).

In this discussion I have dealt mainly with issues of the astrophysics of potential calibration sources (e.g. the modeling of calibrator SEDs, the frequency and identification of multiplicity). However there are potentially other instrument-specific

---

<sup>7</sup>available at <http://vizier.u-strasbg.fr/cgi-bin/VizieR>

<sup>8</sup>available at <http://ad.usno.navy.mil/wds/>

<sup>9</sup>available at <http://astro.estec.esa.nl/Hipparcos/>

factors that should be considered in selecting calibration sources. For instance, for big-aperture interferometers such as VLTI and KI, the Adaptive Optics correction performance will be a function of brightness, and may be a function of color. So it may become necessary to approximately match brightnesses and colors between target and calibrators. Another possible consideration is in the delay coverage of the interferometer for targets at the extremes of declination coverage where small differences in sky position can result in surprisingly large differences in temporal accessibility. Fortunately most planning software (getCal, ASPRO) also includes temporal accessibility as part of the standard feature set.

## References

- Akeson, R.L. *et al.* 2000, ApJ 543, 313.  
Batten, A.H. *et al.* 1989, PDAO 17 1.  
Blackwell, D., and Lynas-Gray, A. 1994, A&A 282, 899.  
Boden, A.F. *et al.* 1998, Proc. SPIE 3350, 872.  
Boden, A.F. 1999, "Elementary Theory of Interferometry", Proc. 1999 Michelson Summer School, (<http://sim.jpl.nasa.gov/michelson/iss1999/index.html>)  
Cox, A.N. *et al.* 1999, Allen's Astrophysical Quantities, AIP Press.  
Duquennoy, A., and Mayor, M. 1991, A&A 248, 485.  
ESA 1997, The Hipparcos and Tycho Catalogues, ESA SP-1200.  
Ghez, A.M. *et al.* 1991, AJ 102, 2066.  
Koresko, C.D. 2000, ApJ 531, L147.  
Marcy, G.W. *et al.* 1997, ApJ 481, 926.  
Mayor, M. and Queloz, D. 1995, Nat 378, 355.  
Mozurkewich, D. *et al.* 1991, AJ 101, 2207.  
Rybicki, G.B. and Lightman, A.P. 1979, Radiative Processes in Astrophysics, John Wiley & Sons.